Force imbalance in lattice Boltzmann equation for two-phase flows

Zhaoli Guo,[1,2,*] Chuguang Zheng,[2] and Baochang Shi[3]

[1]*State Key Laboratory of Enhanced Oil Recovery, Research Institute of Petroleum Exploration and Development, Beijing 100083, China*

[2]*National Laboratory of Coal Combustion, Huazhong University of Science and Technology, Wuhan 430074, China*

[3]*School of Mathematics and Statistics, Huazhong University of Science and Technology, Wuhan 430074, China*

(Received 29 March 2010; revised manuscript received 10 January 2011; published 28 March 2011)

The capability of modeling and simulating complex interfacial dynamics of multiphase flows has been recognized as one of the main advantages of the lattice Boltzmann equation (LBE). A basic feature of two-phase LBE models, i.e., the force balance condition at the discrete lattice level of LBE, is investigated in this work. An explicit force-balance formulation is derived for a flat interface by analyzing the two-dimensional nine-velocity (D2Q9) two-phase LBE model without invoking the Chapman-Enskog expansion. The result suggests that generally the balance between the interaction force and the pressure does not hold exactly on the discrete lattice due to numerical errors. It is also shown that such force imbalance can lead to some artificial velocities in the vicinity of phase interface.

DOI: 10.1103/PhysRevE.83.036707 PACS number(s): 47.11.Qr, 05.20.Dd, 47.55.−t, 68.03.−g

I. INTRODUCTION

Multiphase flows arise in many important scientific and technological applications. Owing to the complex interfacial dynamics involving large space and time scales, it is a rather challenging task to model and simulate such flows. Essentially, the interfacial phenomena in multiphase systems are the natural consequences of microscopic interactions among fluid molecules. Therefore, in principle, multiphase flows can be simulated by numerical methods based on realistic microscopic physics such as molecular dynamics (MD). Indeed, there are ample applications of MD in the study of multiphase flows. Unfortunately, such methods are usually very computationally expensive and consequently become impractical for simulating macroscopic flows. In recent years there has been a trend to construct numerical methods for complex flows based on mesoscopic theories that connect the microscopic and macroscopic descriptions of the dynamics, among which the lattice Boltzmann equation (LBE) [1,2] has received particular attention. Thanks to the kinetic nature of the LBE, intermolecular interactions can be incorporated into a LBE model in a straightforward way so that it can be used to simulate a multiphase system effectively. This feature is also recognized as one of the main advantages of LBE that distinguishes it from other numerical methods, and a number of successful applications of LBE to multiphase systems have been reported [3].

In a multiphase LBE, discrete distribution functions or populations of simulated fluid particles collide and stream on a regular lattice, while the intermolecular interactions are modeled based on different physical pictures. In the earlier color-gradient (CG) LBE models, the interparticle interactions were modeled by a local color gradient associated with the density difference between the two phases [4]. The idea of using an artificial interparticle nearest-neighbor potential to model fluid interactions in the LBE was attributed to Shan and Chen [5], which was similar to the idea used in lattice gas automata [6]. This type of LBE model (SC model) is very popular due to its simplicity in controlling the interaction strengths in the system. Unlike the CG and SC LBE models in which the interactions are constructed heuristically, Swift *et al*. proposed a LBE model by introducing a pressure tensor derived from the free-energy of a multiphase system [7]. The above three types of LBE models have all been applied to a multitude of multiphase problems. However, these models usually involve some heuristic arguments more or less, which may lead to some undesirable artifacts [8,9]. Important advancements were made after the connections between the LBE and the continuous Boltzmann equation were established [10]. It is well understood that it is still a challenging topic to model a two-phase flow in continuum theory. On the other hand, the underlying microscopic interactions in fluids can be effectively modelled in kinetic theory. Therefore, the connection between LBE and kinetic theory can provide some insights as to how to construct consistent LBE models. Indeed, several multiphase LBE models have been successfully developed based on different models of the kinetic theory, such as the modified Boltzmann equation, the Enskog equation, and the Bogoliubov-Born-Green-Kirkwood-Yvon (BBGKY) hierarchy [8,9,11–13]. It should be noted that these models are closely related, particularly in the dealing with the interparticle interactions. Owing to the underlying physics of the based kinetic theories, these LBE models usually possess firm foundations and are consistent with some fundamental requirements such as the thermodynamic consistency and the Galilean invariance.

While the LBE method has great advantages for the simulation of multiphase flows, it also comes with a number of limitations (see, e.g., [14]). A common undesirable feature of multiphase LBE models is the existence of some abnormal velocities near an interface at equilibrium. Physically, the velocity should vanish in an equilibrium system, but it has been observed in many LBE simulations that some small-amplitude flows exist in the vicinity of an interface. Such unphysical velocity, particularly that in the vicinity of a curve interface, is usually termed as "spurious current" or "parasitic current" in the literature, and various attempts have been made to track the origin and reduce the spurious currents. Nourgaliev *et al*. [15] attributed the anomalous velocity to the local violation of

*zlguo@mail.hust.edu.cn

the momentum conservation, and proposed a "multifractional stepping" procedure for the advection operator together with an implicit trapezoidal discretization of the collision operator. Similarly, Cristea and Sofonea [16] also related the origin of the spurious velocity to the discretization of the advection operator, and suggested using a force correction to eliminate it. Wagner [17] pointed out that the discretization errors for the force appearing in the order parameter equation and the momentum equation drove the spurious currents, and demonstrated that the use of potential form for the surface force could remove the spurious currents near a circular bubble to machine accuracy. However, it was found that the numerical stability of this method was unsatisfied. Lee and Fischer [18] proposed an improved version by introducing a mixed difference scheme for discretizing the force in potential form. However, this method does not conserve the mass and momentum during the evolution [14]. Recently, Shan [19] argued that it was the lack of sufficient isotropy in the discretization of the interaction force that caused the spurious currents, and proposed some schemes with higher isotropy. A similar idea was also used in some later studies [20,21]. The above investigations are helpful for better understanding the spurious currents, and the improved LBE schemes were all able to reduce the velocity magnitude.

Spurious currents were also observed in other numerical methods for two phase flows such as volume-of-fluid method, level set method, and front tracking method (see, e.g., [22–24]). In the computational fluid dynamics (CFD) community it has been realized that it is the imbalance between the pressure and interfacial force at discrete level that leads to the abnormal velocities. This should also be the case in LBE models. However, the force balance condition, which is also a necessary condition for vanishing abnormal velocities in LBE, has not been analyzed in the literature. In this work we aim to investigate this problem by performing a detailed analysis of a kinetic-theory based LBE for two-phase flows without invoking the Chapman-Enskog expansion. An explicit expression for the force balance in LBE is derived. It is found that this condition does not hold exactly in general due to numerical errors, which implies that the abnormal velocities near an interface may be an intrinsic nature of LBE.

II. ANALYSIS OF THE LBE FOR A FLAT INTERFACE

We choose the multiphase LBE based on the extended Boltzmann equation as the basis for analysis [8],

$$f_i(\boldsymbol{x}+\boldsymbol{c}_i\delta_t,t+\delta_t)-f_i(\boldsymbol{x},t)=-\frac{1}{\tau}\left[f_i(\boldsymbol{x},t)-f_i^{(eq)}(\boldsymbol{x},t)\right]+\delta_t F_i(\boldsymbol{x},t), \tag{1}$$

for $i=0,\cdots,b-1$, where $f_i(\boldsymbol{x},t)$ is the distribution function at position $\boldsymbol{x}=(x,y,z)$ and time t associate with the discrete velocity $\boldsymbol{c}_i$, $f_i^{(eq)}$ is the equilibrium distribution function given by

$$f_i^{(eq)}=w_i\left[1+\frac{\boldsymbol{c}_i\cdot\boldsymbol{u}}{c_s^2}+\frac{(\boldsymbol{c}_i\cdot\boldsymbol{u})^2}{2c_s^4}-\frac{\boldsymbol{u}\cdot\boldsymbol{u}}{2c_s^2}\right], \tag{2}$$

where w_i is the weight, c_s is a model constant, and ρ and $\boldsymbol{u}$ are the fluid density and velocity, respectively. The forcing term F_i accounts for a body force $\boldsymbol{F}$ and can be expressed as

$$F_i=\left(1-\frac{1}{2\tau}\right)\frac{(\boldsymbol{c}_i-\boldsymbol{u})\cdot\boldsymbol{F}}{c_s^2\rho}f_i^{(eq)}. \tag{3}$$

It is noted that part of F_i can be regrouped into the relaxation term in Eq. (1), which was adopted in some previous works [8,18]. The formulation (3) is identical to that proposed in Ref. [25] after neglecting terms of $O(u^3)$. The force due to intermolecular interactions can be expressed as [8,11]

$$\boldsymbol{F}=\nabla\left(c_s^2\rho-p_0\right)+\rho\kappa\nabla\nabla^2\rho=\nabla\left(c_s^2\rho\right)-\rho\nabla\mu, \tag{4}$$

where p_0 is the thermodynamic pressure dependent on the equation of state, κ is a parameter relating to the surface tension, $\mu=\mu_0-\kappa\nabla^2\rho$ is the chemical potential with μ_0 being the chemical potential in the bulk phase. In some works [17,18], the first equation of (4) is termed as "pressure form" while the second is termed as "potential form." Although the two formulations are totally identical mathematically, their discrete versions may differ slightly due to some discretization errors, and may have significant influences on the spurious currents [17,18].

It should be pointed out that most of the available two-phase LBE models are designed for isothermal flows, which is also the case considered in the present work. Such a model is insufficient to describe the energy transport of the system, and thus the concept of "chemical potential" or other thermodynamic concepts, may lead to some confusions. However, such concepts are still helpful for understanding the structure of phase interfaces in an isothermal system, and may be helpful for improving performances of numerical schemes. For example, Jamet *et al*. have shown that the use of potential formulation in the discretization of the momentum equation can reduce the spurious currents greatly in a finite-volume scheme for isothermal two-phase systems [22], and similar strategies were also employed in some isothermal two-phase LBE models [17,18].

With the presence of the body force the fluid velocity must be defined as

$$\rho\boldsymbol{u}=\sum_i\boldsymbol{c}_i f_i+\frac{\delta_t}{2}\boldsymbol{F},\quad\text{with}\quad\rho=\sum_i f_i. \tag{5}$$

Otherwise one cannot obtain correct hydrodynamic equations [25], and a large spurious current will emerge [19]. Using the Chapman-Enskog expansion, we can derive the hydrodynamic (mass and momentum conservative) equations from the LBE (1) as

$$\frac{\partial\rho}{\partial t}+\nabla(\rho\boldsymbol{u})=0, \tag{6a}$$

$$\frac{\partial(\rho\boldsymbol{u})}{\partial t}+\nabla(\rho\boldsymbol{u}\boldsymbol{u})=-\nabla\left(c_s^2\rho\right)+\nabla\cdot(\rho\nu\boldsymbol{S})+\boldsymbol{F}, \tag{6b}$$

where $S_{\alpha\beta}=\partial_\alpha u_\beta+\partial_\beta u_\alpha$ and ν is the shear viscosity defined by $\nu=c_s^2\rho(\tau-0.5)\delta_t$. These equations are similar to the Navier-Stokes equations for two-phase flows.

In order to understand the origin of the spurious current in LBE, we consider a two-dimensional flat interface parallel to the x direction where the density changes only in the y direction. As such, we can assume that $\boldsymbol{u}=(u_x,u_y)=(0,v)$,

$\boldsymbol{F} = (F_x, F_y) = (0, F)$, and $\partial_x \phi = 0$ for any fluid variable ϕ. We will apply the two-dimensional nine-velocity (D2Q9) LBE model as an example to this problem. In the model the discrete velocities are given by $\boldsymbol{c}_0 = (0,0)$, $\boldsymbol{c}_1 = -\boldsymbol{c}_3 = c(1,0)$, $\boldsymbol{c}_2 = -\boldsymbol{c}_4 = c(0,1)$, $\boldsymbol{c}_5 = -\boldsymbol{c}_7 = c(1,1)$, and $\boldsymbol{c}_6 = -\boldsymbol{c}_8 = c(-1,1)$, with $c = \delta_x/\delta$ being the lattice speed (δ_x is the lattice spacing). Without loss of generality, we will take δ_x, δ_t, and c as the length, time, and velocity units, respectively ($\delta_x = \delta_t = c = 1$). The parameter c_s is $1/\sqrt{3}$ and the weights are $w_0 = 4/9$, $w_{1\sim4} = 1/9$, and $w_{5\sim8} = 1/36$.

For the flat interface, Eq. (6a) reduces to $\partial_y(\rho v) = 0$ at steady state, which gives $v = 0$. Based on this fact, some previous studies claimed that spurious currents would not appear for a flat interface in LBE [19,20]. However, it should be borne in mind that Eq. (6a) is derived from the LBE (1) asymptotically, and the LBE can be viewed as a special finite-difference scheme for solving Eq. (6a). Therefore, the solutions of the LBE and the Navier-Stokes equations may be different. To see this more clearly, we now try to find the analytical solution of the LBE for this flat interface problem without invoking the Chapman-Enskog expansion. In this case the LBE (1) can be written as

$$f_i(\boldsymbol{x} + \boldsymbol{c}_i\delta) = f_i'(\boldsymbol{x}) \equiv f_i(\boldsymbol{x}) - \frac{1}{\tau}\left[f_i(\boldsymbol{x}) - f_i^{(eq)}(\boldsymbol{x})\right] + F_i(\boldsymbol{x}). \tag{7}$$

Particularly, we have $f_i = f_i'$ for $i = 0$, 1, and 3, from which we can obtain that

$$f_{013} \equiv f_0 + f_1 + f_3 = \frac{2}{3}\left(1 - \frac{v^2}{2c_s^2}\right)\left[\rho - \left(\tau - \frac{1}{2}\right)\frac{vF}{c_s^2}\right].$$

With this result and the definitions of ρ and v, i.e.,

$$f_{256} + f_{478} = \rho - f_{013}, \quad (f_{256} - f_{478}) = \rho v - \tfrac{1}{2}F,$$

where $f_{256} \equiv f_2 + f_5 + f_6$ and $f_{478} \equiv f_4 + f_7 + f_8$, we can obtain that

$$f_{256} = \frac{\rho}{6} + \frac{\rho v^2}{2} + \frac{\rho v}{2} - \frac{F}{4} + \left(\tau - \frac{1}{2}\right)\left[1 - \frac{3v^2}{2}\right]Fv, \tag{8a}$$

$$f_{478} = \frac{\rho}{6} + \frac{\rho v^2}{2} - \frac{\rho v}{2} + \frac{F}{4} + \left(\tau - \frac{1}{2}\right)\left[1 - \frac{3v^2}{2}\right]Fv. \tag{8b}$$

In the above equations the terms of $O(v^3)$ comes from that in the forcing scheme Eq. (3). If we take the forcing scheme proposed in Ref. [25], these terms will not appear.

Multiplying 1 and c_{iy} on both sides of Eq. (7) and taking summation over i, respectively, we can obtain mass and momentum conservative equations in discrete form as

$$f_{256}(j+1) + f_{478}(j-1) + f_{013}(j) = \rho_j, \tag{9a}$$

$$f_{256}(j+1) - f_{478}(j-1) = \rho v_j + \frac{\delta}{2}F_j, \tag{9b}$$

where j is the label of the grid number along the y direction. Substituting the expressions of f_{013}, f_{256}, and f_{478} into Eq. (II), we can obtain that

$$-\frac{\rho_{j+1} - 2\rho_j + \rho_{j-1}}{3} + \frac{F_{j+1} - F_{j-1}}{2} = R_1(v_j), \tag{10a}$$

$$-\frac{\rho_{j+1} - \rho_{j-1}}{3} + \frac{F_{j+1} + 2F_j + F_{j-1}}{2} = R_2(v_j), \tag{10b}$$

where R_1 and R_2 are two collective terms of v,

$$\begin{aligned} R_1(v_j) = {} & (\rho_{j+1}v_{j+1} - \rho_{j-1}v_{j-1}) \\ & + (4\tau - 2)(F_{j+1}v_{j+1} - 2F_jv_j \\ & + F_{j-1}v_{j-1}) + O(v^3), \end{aligned} \tag{11a}$$

$$\begin{aligned} R_2(v_j) = {} & (\rho_{j+1}v_{j+1} - 2\rho_jv_j + \rho_{j-1}v_{j-1}) \\ & + \left(\rho_{j+1}v_{j+1}^2 - \rho_{j-1}v_{j-1}^2\right) \\ & + (2\tau - 1)(F_{j+1}v_{j+1} - F_{j-1}v_{j-1}) + O(v^3). \end{aligned} \tag{11b}$$

If we assume $F \sim v$, the leading order of R_1 is $\rho_{j+1}v_{j+1} - \rho_{j-1}v_{j-1}$, and therefore Eq. (10a) can be viewed as a numerical scheme of the partial differential equation (PDE) $\partial_y(\rho v) = \partial_y(F - c_s^2\partial_y\rho)$. Theoretically $F - c_s^2\partial_y\rho = 0$ at equilibrium because the chemical potential μ is a constant in this case [22], and therefore the PDE is the same as the continuum equation (6a) derived from the LBE through the Chapman-Enskog analysis. However, at discrete level the left-hand side of Eq. (10a) may not vanish totally, and thus the arguments about the spurious current based on Eq. (6) may be inaccurate.

Actually, it is noted that $R_1 = R_2 = 0$ if $v = 0$, and therefore we can obtain a force balance or necessary condition for vanishing spurious current,

$$\frac{F_{j+1} - F_{j-1}}{2} = \frac{\rho_{j+1} - 2\rho_j + \rho_{j-1}}{3}, \tag{12a}$$

$$\frac{F_{j+1} + 2F_j + F_{j-1}}{4} = \frac{c_s^2[\rho_{j+1} - \rho_{j-1}]}{2}. \tag{12b}$$

These two equations can be viewed as numerical schemes for the following equations:

$$\partial_y\left(F - c_s^2\partial_y\rho\right) = 0, \quad F - c_s^2\partial_y\rho = 0, \tag{13}$$

which are consistent with each other.

The terms on the left- and right-hand sides of Eqs. (12a) and (12b) are linear combinations of the interaction force and fluid density, respectively. For nonideal gases, it is well understood that the pressure given by the equation of state is usually a nonlinear function of the density that varies nonlinearly in the interfacial region, and so is the interaction force F. Furthermore, because the gradients in the force given by Eq. (4) should be evaluated numerically point by point in the LBE (1), the terms on the left-hand side of Eqs. (12a) and (12b) may involve some terms like ρ_{j+2} and/or ρ_{j-2}, which are absent on the right-hand side. Therefore, Eqs. (12a) and (12a) represent two highly nonlinear algebraic systems of the density ρ on the lattice nodes. An obvious solution of either system is $\rho =$ const, which is unphysical for a two-phase system. It is difficult to give a rigorous mathematical proof whether other nontrivial solutions exist for an arbitrary interaction force F, because the existence of such solutions also depend on the formulations of the force, the numerical discretization schemes, and boundary conditions. Furthermore, even if a nonconstant density profile satisfying Eq. (12) exists theoretically, the LBE solution may still deviate from it due to numerical errors.

The above arguments indicate that the force balance condition (12) does not hold exactly in general at the discrete level, regardless of the force formulations (either pressure form or potential form) and numerical schemes for the gradients. The small force imbalance due to the numerical errors will produce some artificial velocities inevitably. Although the above arguments are made based on the LBE model derived from an extended Boltzmann equation [8], they also apply to other types of LBE models in that their evolution equations can also be reformulated as Eq. (1) with different force formulations [8,9]. It should be noted that the above analysis is based on a one-dimensional flat interface where the finite curvature effects are neglected. For two- or three-dimensional interfaces, the presentence of a finite curvature will make the force balance condition more complicated, but the discrete nature of the LBE as a finite-difference scheme remains unchanged, and discrete errors will still exist inevitably, which will lead to slight force imbalance at the discrete level. In this regard, the main result from the one-dimensional analysis, i.e., artificial velocities in LBE are caused by the force imbalance due to discrete errors, is also applicable to more general cases.

III. NUMERICAL RESULTS

We now carry out some numerical simulations to demonstrate the conclusion. The system considered is a van der Waals fluid whose bulk free energy is given by

$$\psi_0 = \beta(\rho - \rho_l)^2(\rho - \rho_v)^2,$$

where β is a constant relating to the surface tension, ρ_l and ρ_v are the densities of liquid and vapor phases at saturation, respectively. With this free energy, the density across a flat interface at equilibrium is a hyperbolic tangent profile with thickness $D = \sqrt{8\kappa/\beta}/(\rho_l - \rho_v)$, and the surface tension is $\sigma = \sqrt{2\kappa\beta}(\rho_l - \rho_v)^3/6$. The thermodynamic pressure p_0 and chemical potential μ_0 in Eq. (4) can be derived from ψ_0 as

$$p_0 = \rho\partial\psi_0/\partial\rho - \psi_0, \quad \mu_0 = \partial\psi_0/\partial\rho.$$

With this free energy Lee and Fischer reported vanishing spurious currents near a circular droplet [18].

The gradients in the interaction force (4) can be discretized with different schemes. A widely used scheme is the isotropic central scheme (ICS),

$$\nabla_c\phi(\boldsymbol{x}) = \frac{1}{c_s^2}\sum_{i=0}^{b-1} w_i \boldsymbol{c}_i \phi(\boldsymbol{x} + \boldsymbol{c}_i), \tag{14a}$$

$$\nabla_c^2\phi(\boldsymbol{x}) = \frac{2}{c_s^2}\left[\sum_{i=0}^{b-1} w_i \phi(\boldsymbol{x} + \boldsymbol{c}_i) - \phi(\boldsymbol{x})\right], \tag{14b}$$

where ϕ is an arbitrary function. Some other ICS's involving more neighboring grids were also proposed in order to achieve higher isotropy [19]. Lee and Fischer [18] proposed an alternative second-order mixed difference scheme,

$$\nabla_m\phi = \tfrac{1}{2}(\nabla_b\phi + \nabla_c\phi),$$

where

$$\nabla_b\phi(\boldsymbol{x}) = \sum_{i=0}^{b-1} \frac{w_i \boldsymbol{c}_i\,[-\phi(\boldsymbol{x} + 2\boldsymbol{c}_i) + 4\phi(\boldsymbol{x} + \boldsymbol{c}_i) - 3\phi(x)]}{2c_s^2},$$

which is essential a higher order isotropic ICS similar to that proposed in [19]. It should be noted that in the Lee-Fischer method the gradient term $(\boldsymbol{c}_i - \boldsymbol{u})\cdot\nabla\phi$ is calculated as two parts, namely $\boldsymbol{c}_i\cdot\nabla\phi$ and $\boldsymbol{u}\cdot\nabla\phi$. The latter is evaluated using the above mixed scheme, while the former is calculated using a mixed second-order directional finite-difference scheme,

$$\boldsymbol{c}_i\cdot\nabla_m\phi = \tfrac{1}{2}(\boldsymbol{c}_i\cdot\nabla_b\phi + \boldsymbol{c}_i\cdot\nabla_c\phi),$$

where

$$\boldsymbol{c}_i\cdot\nabla_b\phi = \frac{-\phi(\boldsymbol{x} + 2\boldsymbol{c}_i) + 4\phi(\boldsymbol{x} + \boldsymbol{c}_i) - 3\phi(\boldsymbol{x})}{2},$$

$$\boldsymbol{c}_i\cdot\nabla_c\phi = \frac{\phi(\boldsymbol{x} + \boldsymbol{c}_i) - \phi(\boldsymbol{x} - \boldsymbol{c}_i)}{2}.$$

A problem of the Lee-Fischer scheme is that the forcing term does not conserve mass and momentum strictly (i.e., $\sum_i F_i \neq 0$ and $\sum_i \boldsymbol{c}_i F_i \neq \boldsymbol{F}$) due to the different discretization errors in the two parts [20].

Three schemes will be considered according to the treatments of the interaction force, i.e., pressure form with ICS (pressure-ICS), potential form with ICS (potential-ICS), and potential form with the mixed scheme (Lee-Fischer scheme). All simulations are carried out on a $N_x \times N_y = 100 \times 100$ lattice with periodic boundary conditions in both x and y directions. The first test case is a flat interface where the central region ($25 \leqslant y \leqslant 75$) is filled with the liquid and the rest is occupied by the vapor. The saturation densities of the liquid and vapor are set to be $\rho_l = 1.0$ and $\rho_v = 0.2$, respectively.

If initially the density profile is set to be at equilibrium, i.e.,

$$\rho_0(y) = \rho_v + \frac{\rho_l - \rho_v}{2}\left[\tanh(y_1) - \tanh(y_2)\right], \tag{15}$$

with $y_1 = 2(y - 25)/D$ and $y_2 = 2(y - 75)/D$, it is found that the magnitudes of the spurious currents predicted by the three schemes all tend to zero in machine accuracy at steady state. On the other hand, if the initial density distribution is slightly disturbed from the equilibrium, $\rho_0(y) \to \rho_0(y)(1 + 0.01r)$, where r is a random number distributed uniformly between -0.5 and 0.5, the magnitudes of the spurious currents do not vanish for both the potential-ICS and the Lee-Frischer scheme, but the pressure-ICS yields nearly vanishing spurious currents to machine accuracy in this case, as shown in Fig. 1(a) where the average kinetic energy $E = \int \frac{1}{2}\rho|\boldsymbol{u}|^2 d\boldsymbol{x}$ is plotted. Figure 1(b) shows, however, that only the Lee-Fischer scheme can preserve the exact density profile with correct liquid and vapor densities. It is found that, however, the total mass does not conserve during the evolution of the Lee-Fischer scheme (up to 0.1%), and the deviation increases with the magnitude of the initial perturbations.

The interfaces predicted by both the potential-ICS and pressure-ICS are almost identical and much wider than the theoretical one ($D = 4$), and the liquid and vapor densities deviate significantly from the desired values. The deviations are found to be dependent on the parameters β and κ, and so are the spurious currents. In Fig. 2 the density profile and average kinetic energy of the pressure-ICS with different values of β are shown. Here the parameter κ is changed so that the interfacial thickness D is fixed ($D = 4.0$). It seen

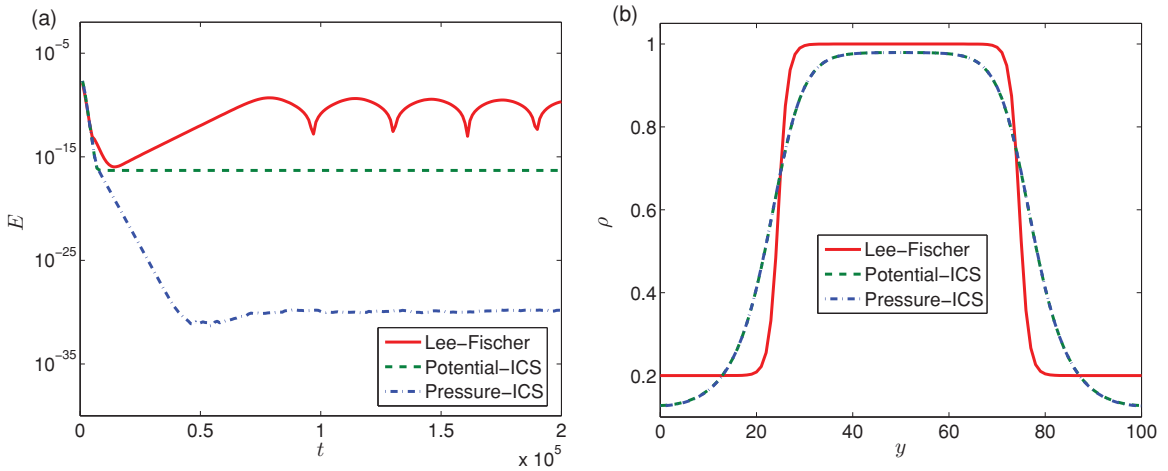

FIG. 1. (Color online) Time evolution of the average kinetic energy (a) and the density distribution across the interface (b) simulated by the LBE with the Lee-Fischer scheme, potential-ICS, and pressure-ICS. The maximum magnitudes of the spurious velocities are 2.66×10^{-5}, 1.28×10^{-8}, and 3.38×10^{-15} for the three schemes, respectively ($\tau = 1.25$, $\beta = 0.01$, and $\kappa = 0.0128$).

from Fig. 2(a) that the deviation of the density profile of the pressure-ICS from the theoretical one given by Eq. (15) increases with increasing β, particularly in the vapor phase. Figure 2(b) shows the same trend of the average kinetic energy, which also indicates the dependence of the spurious current on the parameter β. In general, spurious currents are weak at small values of β, but in such cases both the vapor density and the interfacial thickness show significant deviations from the physical ones. We also tested the spurious currents of the pressure-ICS with fixed κ or β. As seen from the time histories of the average kinetic energy shown in Figs. 3(a) and 3(b), the spurious currents do not vanish in the cases considered, and the magnitude of the spurious currents decreases with increasing κ as $\beta = 0.1$, while increases with increasing β as $\kappa = 0.01$. The velocity profiles at steady state are shown in Figs. 3(c) and 3(d). It is observed that the velocity keeps at two different constant values in the bulk liquid and vapor phases in each case, respectively, and changes smoothly across the interfacial region. The difference between the two bulk velocities varies with κ and β, i.e., increases with decreasing κ and increasing β. These characteristics are also clearly seen from the flow patterns shown in Figs. 3(e) and 3(f).

It is noted that in some previous studies large spurious currents for a flat interface were also observed for the Shan-Chen two-phase model [15,16]. It was argued that these unphysical velocities were due to the incorrect definition of velocity [19], which should be defined by the average of the momenta before and after the collision as given by Eq. (5). However, even with a correctly defined velocity, spurious velocities do not necessarily vanish although the magnitude may be significantly reduced. For example, in Ref. [16] a method that uses an ad hoc extra correction term was proposed to erase spurious currents in the Shan-Chen model. This method "is clearly equivalent to averaging pre-collisions and post-collisions momentum in the SC model" [20]. With this technique, the magnitude of the spurious currents for a flat

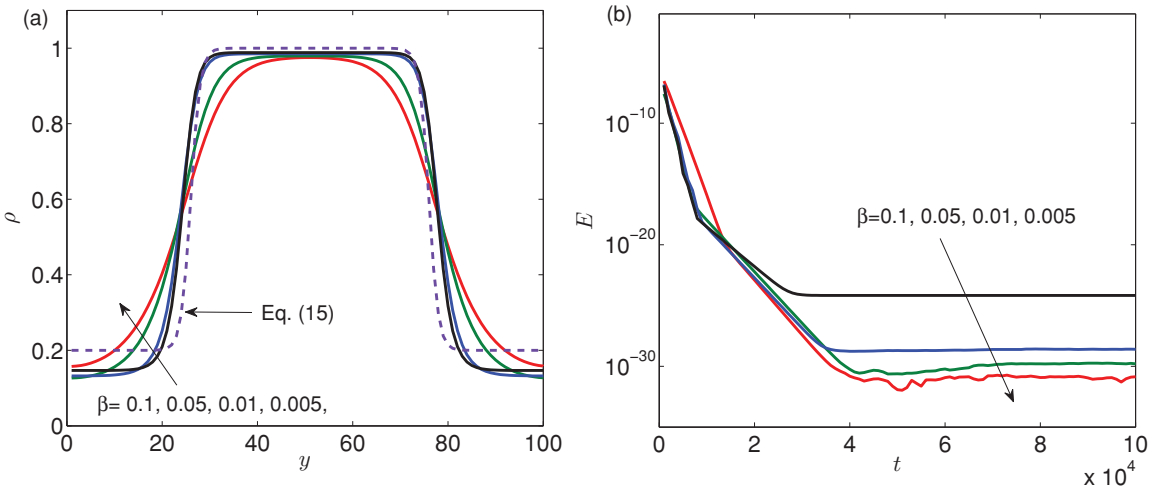

FIG. 2. (Color online) Density profile (a) and time history of the average kinetic energy (b) of the pressure-ICS with different values of β at $D = 4.0$. The maximum magnitude of the spurious currents are of order 10^{-15}, 10^{-15}, 10^{-14}, and 10^{-12} for $\beta = 0.005, 0.01, 0.05$, and 0.1, respectively.

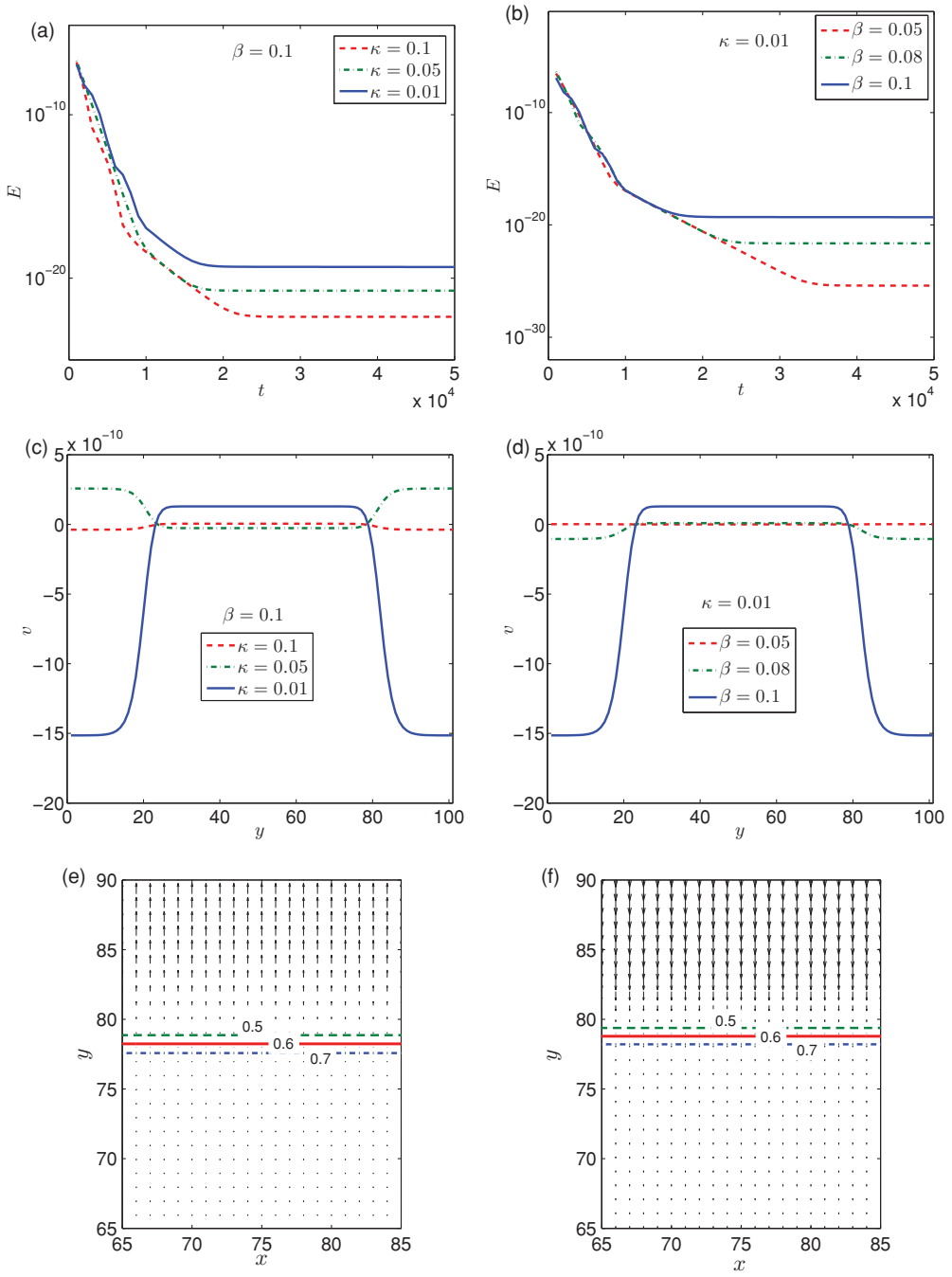

FIG. 3. (Color online) Simulation results of the pressure-ICS with different β and κ. (a) and (b): time history of the average kinetic energy; (c) and (d): steady velocity profile; (e) and (f): flow patterns with $(\beta,\kappa) = (0.1,0.05)$ and $(\beta,\kappa) = (0.01,0.1)$, respectively. The velocity vectors in (e) and (f) are magnified by 3×10^9 and 1×10^9, respectively, and the lines are the density contours.

interface reduced from 10^{-2} to 10^{-6}. We also simulated the flat interface problem using the Shan-Chen model with the correctly defined velocity and obtained similar observations.

In the second test case a liquid droplet with radius 25 is initialized at the center of the 100×100 domain. In this case it is observed that the spurious currents predicted by the Lee-Fischer scheme vanish if the droplet is initialized at equilibrium, but the magnitudes of the spurious currents predicted by the potential-ICS and pressure-ICS are both in the order of 10^{-5} (not shown here). On the other hand, if the equilibrium is disturbed by a small perturbation similar to that in the first test case, nonvanishing currents appear in the final steady state for all of the three schemes. Figure 4 shows the decaying process and density profiles at steady state. It is again observed that only the Lee-Fischer scheme gives the intended density profile, while the other two schemes both fail to predict correct density distributions. However, violation of mass conservation is still observed for the Lee-Fischer scheme.

The above numerical results confirm the theoretical arguments that the nonlinearity of the intermolecular forces

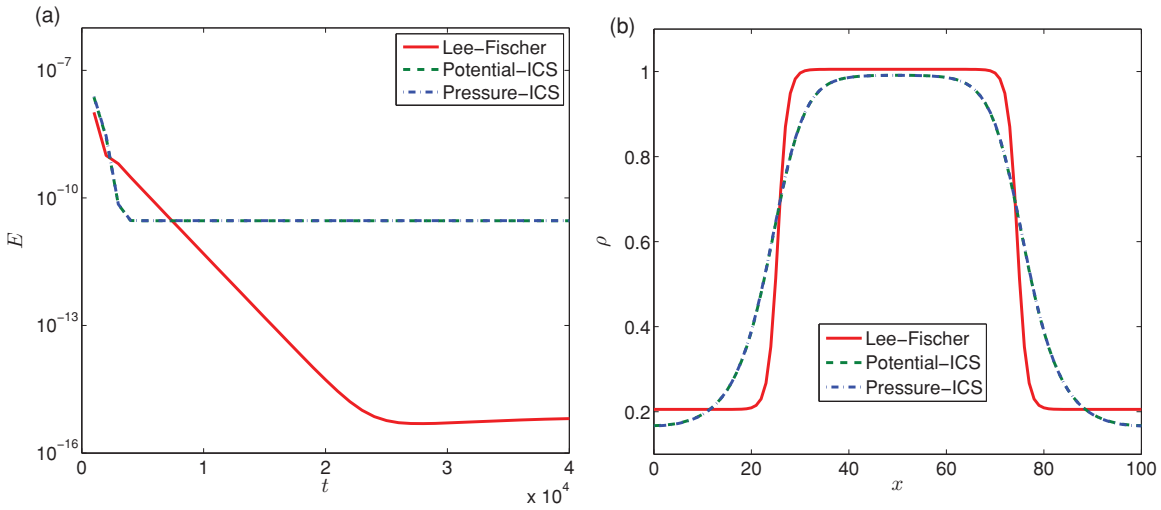

FIG. 4. (Color online) The same as in Fig. 1 but for the droplet system. The maximum magnitudes of the spurious velocities are 5.0×10^{-8}, 4.13×10^{-5}, and 4.16×10^{-5} for the Lee-Fischer scheme, potential-ICS, and pressure-ICS, respectively.

which makes it very difficult (if not impossible) to reach the force balance at discrete level associated with the lattice, and this imbalance will produce some artificial velocities near an interface, which generally cannot be completely removed within the present LBE framework.

IV. SUMMARY

In this study, we performed a theoretical analysis of force balance between pressure and interaction force in two-phase LBE for a simple flat interface without invoking the Chapman-Enskog expansion method. An explicit expression for force balance condition is obtained. Generally this condition could not be fulfilled at the discrete level due to numerical errors. Such force imbalance will lead to some artificial velocities near an interface. Although the analysis is made for a flat interface, the conclusion is also applicable to other cases. The result also implies that the artificial velocity may be an intrinsic nature of the LBE. Numerical tests of the planar interface and the circular droplet problems for three different LBE schemes confirmed the theoretical analysis.

We would like to point out that force balance may be achieved at discrete level if a staggered grid is used, as shown by Jamet *et al*. [22]. In this method, the spatial gradients in pressure, density, and velocity are all discretized using some second-order schemes based on a staggered grid so that the pressure and interfacial force are balanced at a discrete level. As a result, the spurious currents vanished totally to machine accuracy. On the other hand, it is known that in LBE the accuracy of velocity is of second order while the pressure is of first order [26], therefore, it would be a possible way to develop two-phase LBE models with vanishing spurious currents by employing a nonstandard lattice together with an improved evaluation of pressure field.

ACKNOWLEDGMENTS

Z.L.G acknowledges the support by the National Natural Science Foundation of China (10972087) and the Program for NCET in University (NCET-07-0323). The work is also supported by the National Basic Research Programme of China (2011CB707300).

[1] R. Benzi, S. Succi, and M. Vergassola, Phys. Rep. **222**, 145 (1992); S. Chen and G. D. Doolen, Annu. Rev. Fluid Mech. **30**, 329 (1998); C. K. Aidun and J. R. Clausen, Annu. Rev. Fluid Mech. **42**, 439 (2010);

[2] S. Succi, *The Lattice Boltzmann Equation for Fluid Dynamics and Beyond* (Oxford University Press, Oxford, 2001).

[3] F. J. Alexander, S. Chen, and D. W. Grunau, Phys. Rev. B **48**, 634 (1993); X. He, S. Chen, and R. Zhang, J. Comput. Phys. **152**, 642 (1999); I. Ginzburg and K. Steiner, *ibid*. **185**, 61 (2003); A. J. Briant, A. J. Wagner, and J. M. Yeomans, Phys. Rev. E **69**, 031602 (2004); R. Benzi, L. Biferale, M. Sbragaglia, S. Succi, and F. Toschi, *ibid*.**74**, 021509 (2006); C. Pan, M. Hilpert, and C. T. Miller, Water Resour. Res. **40**, W01501 (2004).

[4] A. K. Gunstensen, D. H. Rothman, S. Zaleski, and G. Zanetti, Phys. Rev. A **43**, 4320 (1991).

[5] X. Shan and H. Chen, Phys. Rev. E **47**, 1815 (1993).

[6] H. Chen, S. Chen, G. D. Doolen, Y. C. Lee, and H. A. Rose, Phys. Rev. A **40**, 2850 (1989).

[7] M. R. Swift, W. R. Osborn, and J. M. Yeomans, Phys. Rev. Lett. **75**, 830 (1995).

[8] X. He, X. Shan, and G. D. Doolen, Phys. Rev. E **57**, R13 (1998).

[9] L.-S. Luo, Phys. Rev. Lett. **81**, 1618 (1998); Phys. Rev. E **62**, 4982 (2000).

[10] T. Abe, J. Comput. Phys. **131**, 241 (1997); X. He and L.-S. Luo, Phys. Rev. E **55**, R6333 (1997); X. Shan and X. He, Phys. Rev. Lett. **80**, 65 (1998).

[11] X. He, S. Chen, and R. Zhang, J. Comput. Phys. **152**, 642 (1999).

[12] X. He and G. D. Doolen, J. Stat. Phys. **107**, 309 (2002).

[13] N. S. Martys, Int. J. Mod. Phys. C **10**, 1367 (1999); Q. Zou and X. He, Phys. Rev. E **59**, 1253 (1999); Z. L. Guo and T. S. Zhao, *ibid*. **68**, 035302(R) (2003).
[14] D. Chiappini, G. Bella, S. Succi, F. Toschi, and S. Ubertini, Commun. Comput. Phys. **7**, 423 (2010).
[15] R. R. Nourgaliev, T. N. Dinh, and B. R. Sehgal, Nucl. Eng. Des. **211**, 153 (2002).
[16] A. Cristea and V. Sofonea, Int. J. Mod. Phys. C **14**, 1251 (2003).
[17] A. J. Wagner, Int. J. Mod. Phys. B **17**, 193 (2003).
[18] T. Lee and P. F. Fischer, Phys. Rev. E **74**, 046709 (2006).
[19] X. Shan, Phys. Rev. E **73**, 047701 (2006).
[20] M. Sbragaglia, R. Benzi, L. Biferale, S. Succi, K. Sugiyama, and F. Toschi, Phys. Rev. E **75**, 026702 (2007).
[21] C. M. Pooley and K. Furtado, Phys. Rev. E **77**, 046702 (2008).
[22] D. Jamet, D. Torres, and J. U. Brackbill, J. Comput. Phys. **182**, 262 (2002).
[23] Y. Renardy and M. Renardy, J. Comput. Phys. **183**, 400 (2002).
[24] R. Scardovelli and S. Zaleski, Ann. Rev. Fluid Mech. **31**, 567 (1999).
[25] Z. L. Guo, C. G. Zheng, and B. C. Shi, Phys. Rev. E **65**, 046308 (2002).
[26] M. Junk and A. Klar, SIAM J. Sci. Comput. **22**, 1 (2000); M. Junk, A. Klar, and L.-S. Luo, J. Comput. Phys. **210**, 676 (2005).